12

Mechanical Properties of Kaolin-Base Ceramics During Firing

Igor Štubňa[1], Anton Trník[1,2], František Chmelík[3] and Libor Vozár[1]
[1]*Department of Physics, Constantine the Philosopher University, Nitra,*
[2]*Department of Materials Engineering and Chemistry,*
Czech Technical University, Prague,
[3]*Department of Physics of Materials, Charles University Prague, Prague*
[1]*Slovakia*
[2,3]*Czech Republic*

1. Introduction

Firing of silicate ceramics, which are made of clays with high contents of kaolinite, transforms a green body into a ceramic product [1, 2]. The green body exhibits significant changes of its properties resulting from dehydration at low temperatures, phase changes during dehydroxylation and high-temperature reactions, and densification during sintering [3, 4]. All these changes significantly influence mechanical properties of the fired body as well as its other physical properties.

To save time and energy, it is desirable to conduct the firing in the shortest time possible without damage to the fired ceramic body. Calculating the safe upper limit of the heating or cooling rate of the large ceramic bodies (e.g. high-voltage insulators) is a complex task that requires knowing five material quantities: mechanical strength (MOR), Young's modulus (YM), Poisson's ratio, thermal conductivity, and coefficient of the linear thermal expansion (CLTE). All of these quantities must have to be known as functions of the actual temperature at the firing. The upper limit of the heating rate according to [2] is

$$v_{\max} = \frac{\sigma_f (1-\mu)\lambda}{A\alpha E r^2 c \rho}\ , \tag{1}$$

where σ_f is MOR, μ is Poisson's ratio, λ is thermal conductivity, A is the shape factor of the ceramic body, α is CLTE, E is YM, r is the characteristic dimension of the body, c is volumetric heat capacity and ρ is the volume mass density.

The relationships between the temperature and these qualities (MOR, YM, CLTE, μ and λ) can be identified only using experimental approach despite of some theoretical connection between YM and CLTE or between YM and MOR. These theoretical relationships were derived for simple materials and they are only very approximately applicable to complex multiphase material as kaolin-base ceramics. For thin-wall ceramic bodies such as whiteware, a more simple method based on thermodilatometric results can be used for control of the firing [5].

This chapter is devoted to the development of the two most important mechanical parameters, MOR and YM of the green ceramic material during heating and cooling stages of the firing, with the exception of the highest temperature region where the body becomes partially plastic. Poisson's ratio $\mu = (E/2G) - 1$, where E is YM and G is the elastic shear modulus, can be easily calculated if μ at the room temperature is known. The relationships between YM or shear modulus and the temperature during firing can be assumed as qualitatively identical, i.e. $\mu \approx const$ during the all firing.

2. Experimental

2.1 Samples

Samples from quartz porcelain mixture for the modulated-force thermomechanical analysis (mf-TMA) and measuring MOR were made from 50 % kaolin and clay, 25% quartz and 25% feldspar. The mixture was ground and sieved on a 100 mesh/mm² sieve and turned into a plastic material. Then cylindrical samples (diameter 11 mm) were made with the laboratory vacuum extruder. The samples were dried in the open air and finally content ~1 wt.% of the physically bounded water.

2.2 Modulated force thermomechanical analysis (mf-TMA)

The mf-TMA is an effective experimental method to determine temperature dependence of YM of ceramics [6]. Most of the technical solutions of the method are based on continual measuring the resonant frequency of the sample during a defined temperature regime. The resonant frequency f, the volume mass density ρ, and the sample dimensions (length l and diameter d) serve for the calculation of YM [7, 8]

$$E = 1.12336\left(\frac{l^2 f}{d}\right)^2 \rho T \tag{2}$$

Here, T is a correction coefficient, which should be used if $l/d < 20$. Since the ratio for the used samples $l/d = 15 < 20$, and assuming Poisson's ratio $\mu = 0.2$, the coefficient T = 1.06821 can be determined from the table given in [9].

Since the mass and the dimensions of the green sample are not constant during firing, to obtain the correct value of Young's modulus at the actual temperature t, the mass and the dimensions at the actual temperature t should be substituted into Eq. (2). Then we obtain

$$E(t) = 1.52782\frac{m_0\left(1+\frac{\Delta m(t)}{m_0}\right) l_0^3 f^2(t)}{d_0^4\left(1+\frac{\Delta l(t)}{l_0}\right)} . \tag{3}$$

Relative changes in the mass $\Delta m(t)/m_0$ and dimensions $\Delta l(t)/l_0$ must be determined from the results of thermodilatometric (TDA) and thermogravimetric (TGA) analyses. The values m_0 and l_0 are the initial mass and length of the sample at room temperature. If Eq. (3) is used, simply considering $\Delta m(t) = 0$ and $\Delta l(t) = 0$, a certain error arises. Its relative value for measuring the green sample is shown in Fig. 1.

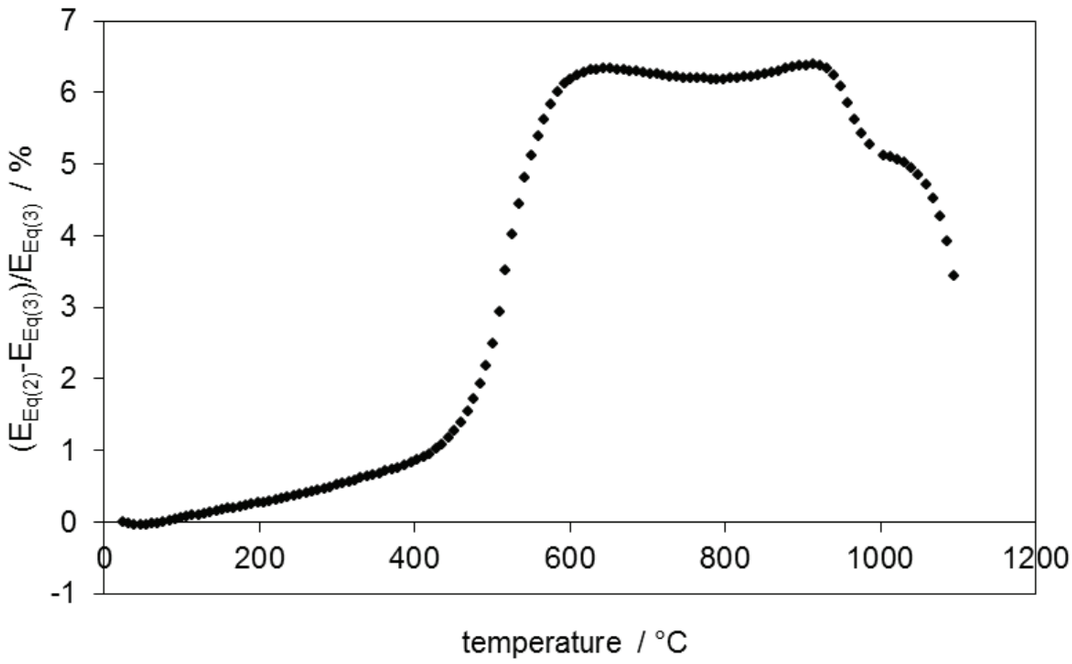

Fig. 1. Relative error $(E_{Eq.(2)} - E_{Eq(3)}) / E_{Eq(3)}$ originated from neglecting the mass and dimensions changes of the sample

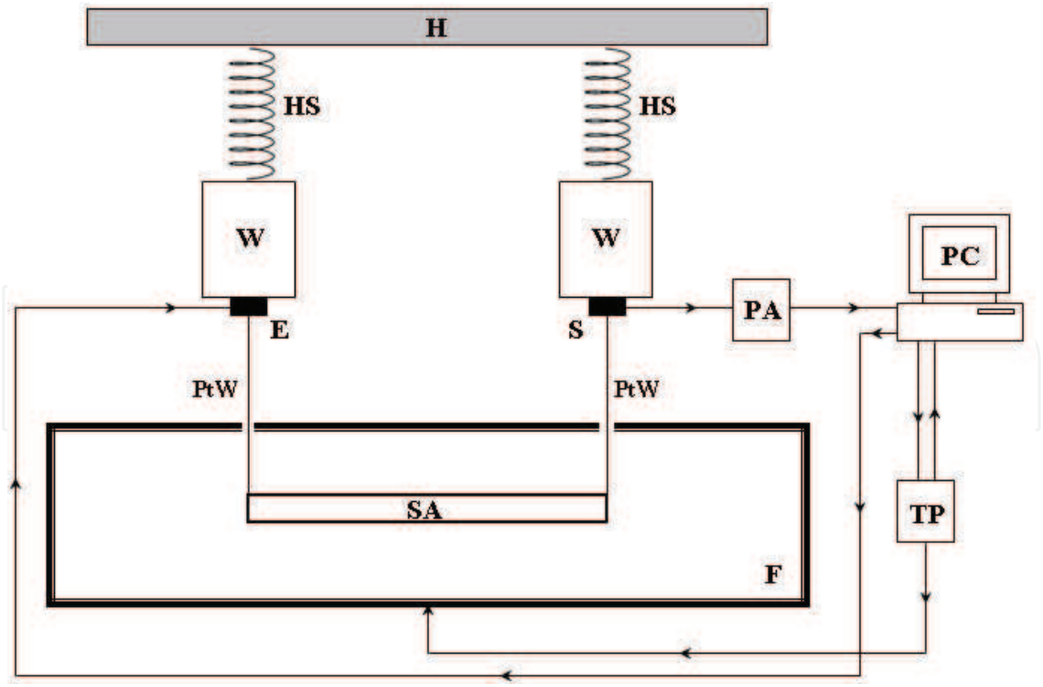

Fig. 2. A scheme of the apparatus for measuring YM.
H – frame, HS – helical spring, W – weight, E – exciter, PtW – platinum wire, S – sensor, PA – preamplifier, SA – sample, F – furnace, PC – computer, TP – temperature programmer

The apparatus for measuring Young's modulus of ceramics at higher temperatures has to satisfy several requirements: a) the sample must be adequately large because some ceramic materials are inhomogeneous and contain crystals of different minerals, glassy phase, and pores; b) green ceramic material is brittle and soft and its mechanical strength is low, and c) the dimensions of the sample contract by up to 8 – 12 % during sintering. We designed an apparatus that satisfies these requirements, see Fig. 2 [10]. It is based on the chart showed in [7, 8] and, in more detail, in [11]. A sample placed horizontally in a furnace is suspended on thin platinum wires (∅0.15 mm) which connect the sample with exciter and sensor located outside the furnace. For the measurement of the sample temperature we use the thermocouple Pt-PtRh10. Its hot ending is in the vicinity of the sample and the cold endings are connected to the temperature programmer.

2.3 Measurement of MOR

Measurements at high temperatures are energy and time-consuming. To make a measurement of MOR more effective, a new apparatus with a heated magazine for 10 samples was designed (Fig. 3). It allows testing of these samples in one heating cycle from 20 to 900 °C using the three-point-bending method.

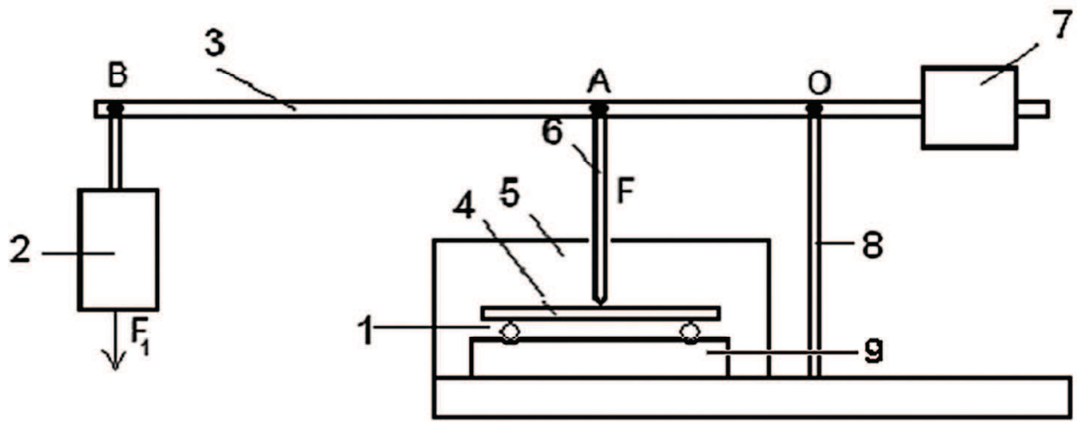

Fig. 3. Apparatus for measuring MOR.
1- supports, 2 - dynamometer, 3 - lever, 4 - sample, 5 - furnace, 6 - alumina rod,
7 - counterweight, 8 – frame, 9 – alumina brick

Temperature of the samples changed linearly at the rate of 5 °C/min. When the temperature reached a chosen value, one sample was broken. The next sample was broken at the next chosen temperature, etc. The loading force increased linearly with a rate of 2 N/s. If the three-point-bending is used, MOR can be calculated from a formula [12]

$$\sigma_f = \frac{8lF_f}{\pi d^3} \tag{4}$$

where d is the diameter of the sample, l is the span between the supports and F_f is the force at the moment of the rupture. However, thermal expansion of the sample diameter $\Delta d(t)$ and the span between supports $\Delta l(t)$ must be taken into account at elevated temperatures. Then Eq. (4) obtains the form

$$\sigma_f(t) = \frac{8[l_0 + \Delta l(t)]}{\pi[d_0 + \Delta d(t)]^3}[aF_{1f}(t) + F_2] \ , \tag{5}$$

Where d_0 and l_0 are the diameter and the span at room temperature, a is a constant of the lever mechanism, $F_{1f}(t)$ is the force registered at the moment of the rupture and F_2 is a small known initial pre-loading force.

3. Heating stage of firing

During heating, several important processes take place in ceramic material. To understand them in more detail it is useful to perform thermal analyses, mainly TGA, DTA and TDA. Their results are shown in Fig. 4 and Fig. 5. Both curves depicted in Fig. 4, TGA and DTA, are of a typical shape for kaolin base ceramics. Since the sample was not fully dried, some physically bounded water was present at the surface defects on walls of kaolinite crystals [13] and in micropores, which caused a subsequent loss of the sample mass at the lowest temperatures. This process is endothermic as confirmed by DTA.

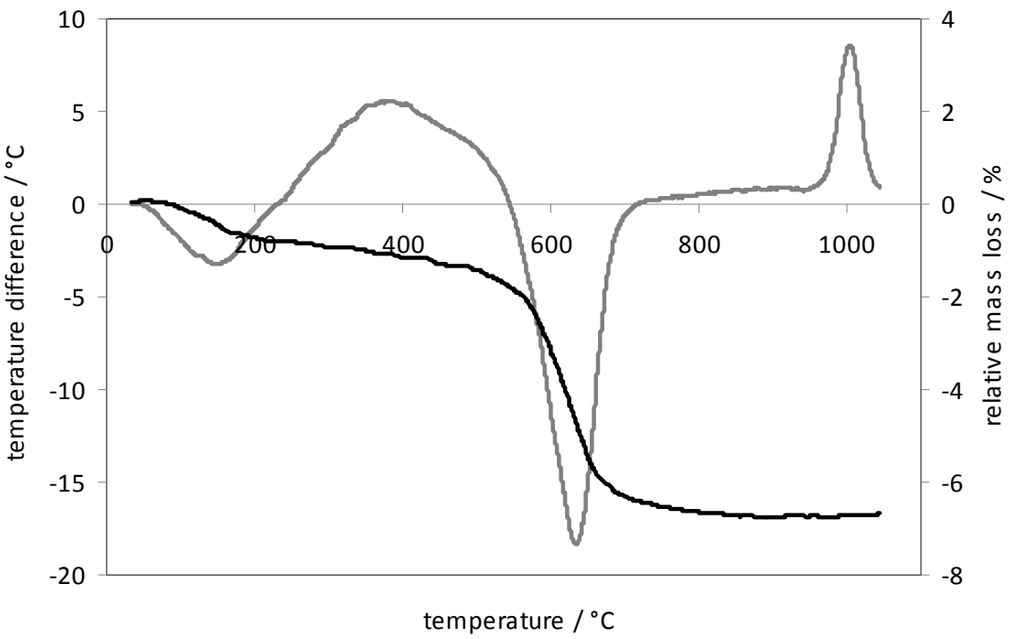

Fig. 4. Relative mass loss (black line) and DTA (gray line)

Fig. 5 and Fig. 6 show the results of TDA and mf-TMA of the green porcelain sample reflecting the same processes as Fig. 4. Comparing Fig. 5 to Fig. 6, the rule "the higher thermal expansion, the lesser YM" is not fulfilled in the temperature range of 20 – 200 °C. Here, two concurrent mechanisms appear. The first is the escaping of the physically bound water from the finest pores and the surface of crystals. This leads to a) a closer contact between crystals and, thereby, to an increasing YM and b) to a small contraction of the sample. Simultaneously, thermal expansion makes YM lower and the dimensions of the sample larger. The net effect of these phenomena demonstrates itself as a steep growth of YM and as a very moderate deceleration of the thermal expansion up to 120 °C.

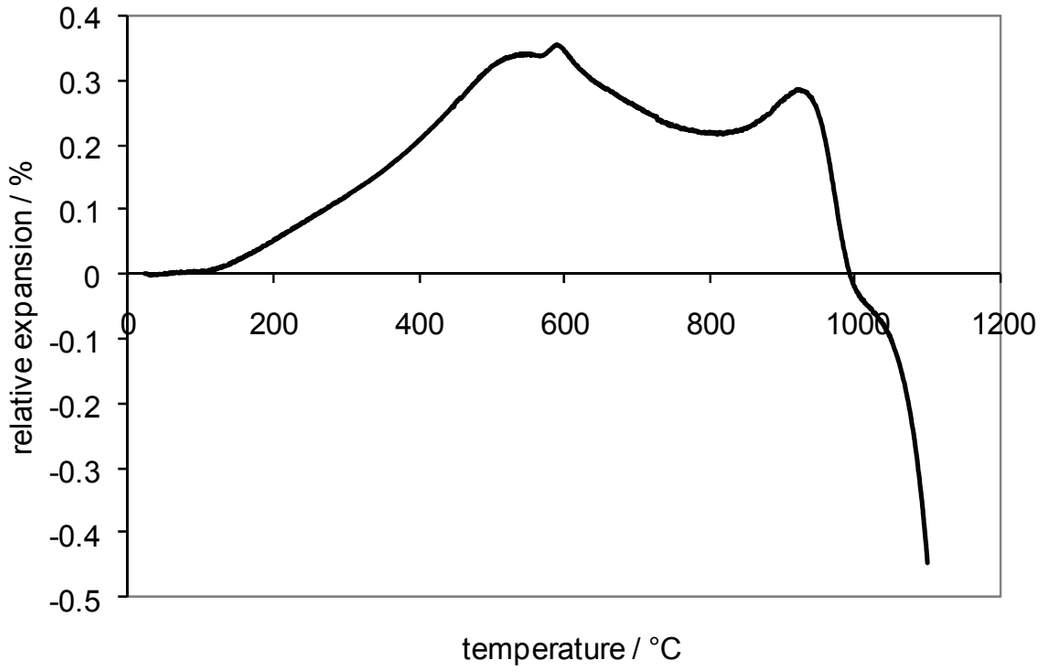

Fig. 5. Thermodilatometric curve of the green sample during heating

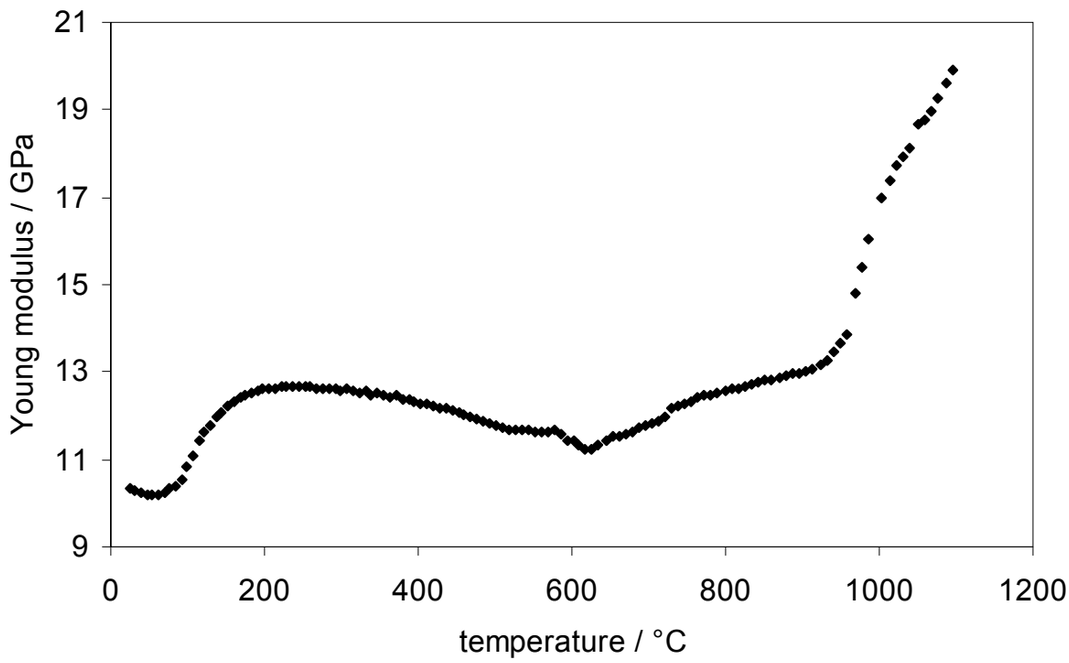

Fig. 6. The results of mf-TMA - Young modulus (calculated according to Eq. (3)) versus temperature

After removing the weakly bound physically water, the sample loses the rest of this water and a very small amount of the organic material, see TGA in Fig. 4. The course of the dilatometric curve represents a simple thermal expansion, as shown in Fig. 5. The values of the thermal expansion increase up to ~500 °C when dehydroxylation occurs, which leads to a contraction of the sample and dropping of its mass. Following the escape of the physically bound water, there is no further change in the structure and composition. Hence, above 200 °C both TDA and mf-TMA results approximately satisfy the rule "the higher thermal expansion, the lesser YM" as long as dehydroxylation emerges at ~450 °C. This process is exhibited in different ways for mf-TMA and TDA. The TDA reflects a) shrinkage of the kaolinite crystals as the result of escaping the crystalline water from their octahedral sheets and b) thermal expansion of the feldspar and quartz.

The mf-TMA is a complex result of four phenomena: a) creation of defects in the kaolinite crystals interiors (which makes YM lower), b) probably the beginning of the solid phase sintering (which makes YM higher), c) loss of the sample mass (which makes YM lower) and d) shrinkage of the sample dimensions (which makes YM higher).

We can conclude that the thermodilatometric behavior of the sample during dehydroxylation is determined primarily by the dehydroxylation process in the kaolinite crystals. The elastic behavior is determined mainly by improving the contacts between the crystals as a consequence of the solid phase sintering. Dehydroxylation plays a minor role in the mf-TMA results (except at a short temperature interval 550 – 620 °C). The temperature interval of dehydroxylation is considered a critical stage of the firing process. It is known that an inadequately high rate of heating or cooling leads to cracking of the ceramic body. This was studied in detail on large cylindrical samples in the dehydroxylation region [14].

The $\alpha \rightarrow \beta$ transition of quartz takes place in the dehydroxylation background, and in spite of a relatively large content of quartz in the sample (25 wt.%), the transition proves only with a small peak at ~570 °C on both curves, TDA and mf-TMA.

Thermal expansion after the completion of dehydroxylation ends at temperature ~950 °C when the collapse of the metakaolinite lattice accompanied by a rapid shrinkage appears. Identically, there is a steep increase in YM in response to a faster solid state sintering and the new structure. A typical exothermic peak on the DTA curve at 1000 °C is characteristic for this process.

Mechanical strength (Fig. 7) approximately follows the course of mf-TMA in Fig. 6. As our preliminary (not yet published) results show, MOR slightly increases in the interval 20 – 200 °C. However, MOR is much more sensitive to defects created by dehydroxylation. Its values run through a clear minimum at ~450 °C. Very similar results were published in [15]. An increase of MOR during the continuing dehydroxylation (above 450 °C) as well as insignificant decrease of YM (Fig. 6) and of the sound velocity (Fig. 8) during dehydroxylation are not easy to explain. Other constituents (quartz and feldspar) do not lose their mechanical properties, and metakaolinite must be considered a mechanically weak material because of the high concentration of defects [16]. The structure of metakaolinite does not change until ~950 °C, so the effect of the MOR increase should be attributed to improving the interfaces between metakaolinite crystals. Solid phase sintering could be a possible relevant mechanism.

It is interesting to compare the results of mf-TMA of the green porcelain sample (Fig. 6) to mf-TMA of kaolin (Fig. 8) [17]. Sound velocity c is related to YM by formula $c^2 = E / \rho$; therefore the temperature dependence of YM and the sound velocity are similar. Comparing

Fig. 6 with Fig. 8 we can conclude that the changes of YM in the three-axial porcelain mixture are predominantly caused by the changes in the kaolin phase and the kaolin crystals interfaces. The same can be stated about MOR. We also made some trial measurements of the acoustic emission during heating. Weak signals were monitored at the temperature range of 250 – 650 °C, which is in accordance with the results of mf-TMA.

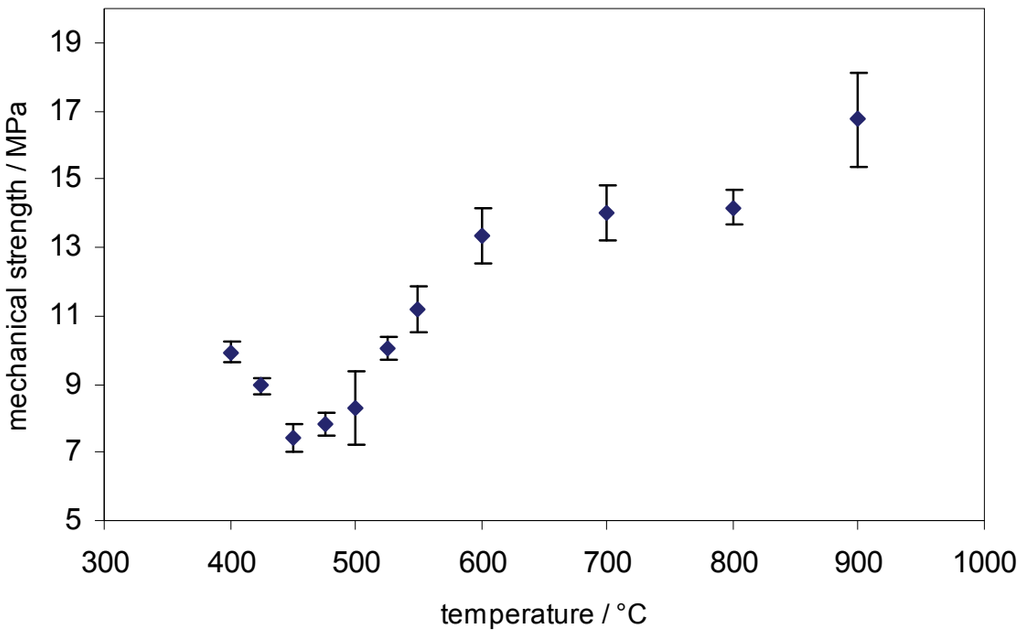

Fig. 7. Mechanical flexural strength measured during heating stage of the firing

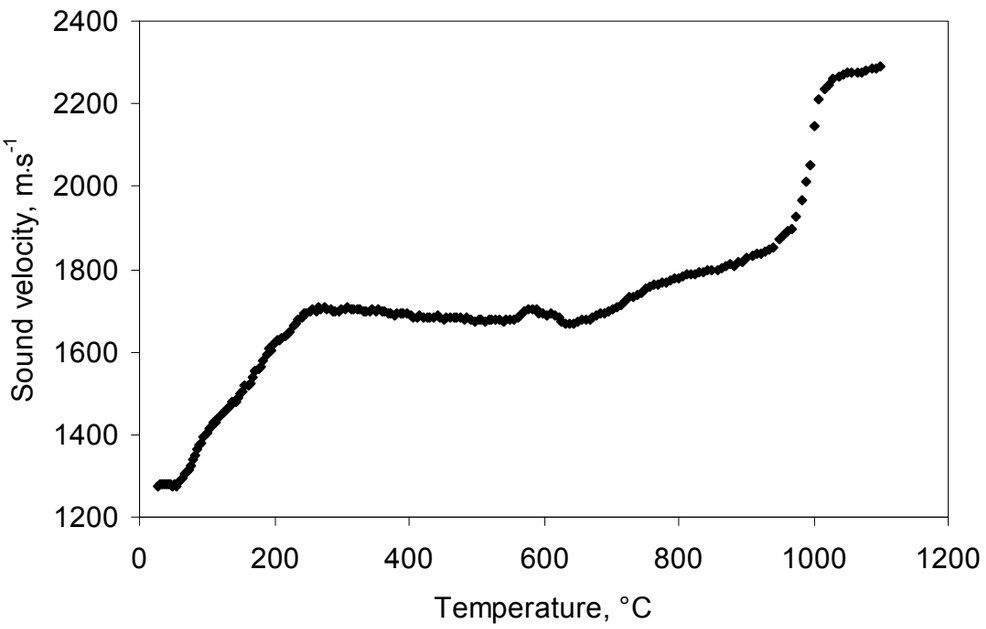

Fig. 8. Sound velocity of kaolin vs. temperature

In theory, the direct implication of Hooke's law is that the relationship between MOR and YM is linear. As can be seen in Fig. 6 and Fig. 7, the courses of YM and MOR are similar, which confirms this theoretical assumption. But there is a considerable scatter of points in this relationship, see Fig. 9, which allows only for a rough estimation of MOR from YM [18].

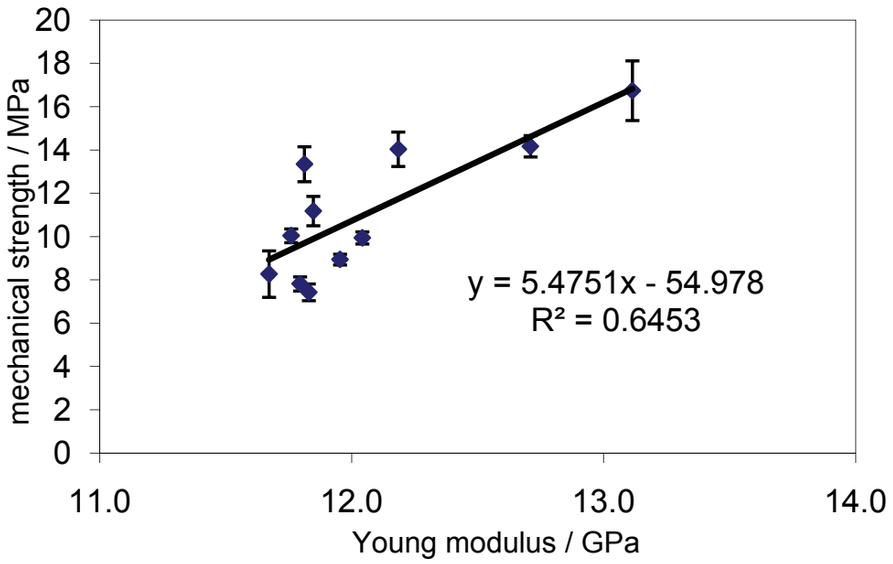

Fig. 9. Relationship between mechanical strength and Young modulus measured at the actual temperature

4. Cooling stage of firing

During heating of the ceramic body from ~1150 °C up to the maximum firing temperature, mullite is created, feldspar melts, the glassy phase occurs and the liquid phase sintering runs. The ceramic body losses elastic properties and becomes plastic. Shrinkage of the sample volume is significant, porosity decreases to a low value [3, 4, 19]. When the body cools down, a viscosity of the glassy phase increases and elastic properties progressively restore. The ceramic material becomes a porcelain.

Numerous studies deal with the influence of the unsolved quartz grains in the porcelain structure. It is recognized that residual quartz grains have a negative influence on the strength of the porcelain. The primary problems associated with quartz in electroporcelain and the ways to decrease the negative effects of quartz were recently described by J. Liebermann [20, 21, 22]. It is commonly believed that the relatively large volume change accompanying the $\beta \rightarrow \alpha$ transformation of the unsolved quartz grains ($\Delta V/V$ = –0.68 % for free quartz grain) is the basic source of microcracking. Investigations performed at room temperature with the help of the electron or light microscopy show circumferential microcracks and (less often) microcracks in quartz grains, see Fig. 10. Based on the model of quartz grain with glassy cladding and the thermodilatometric results (as depicted in Fig. 11), the cooling interval can be divided in two parts. Above 570 °C, the volume of the quartz grain remains approximately constant, and the glassy cladding tends to contract its volume.

The grain is under the compressive stress and no circumferential cracks can arise. But in the narrow temperature interval around the $\beta \rightarrow \alpha$ transition of quartz, the quartz grain volume rapidly contracts and the circumferential microcracks can appear around the grain. The microcracks are the result of the release of the mechanical stress caused by the difference in the thermal expansion between the quartz grains and the glass matrix [21, 23, 24, 25].

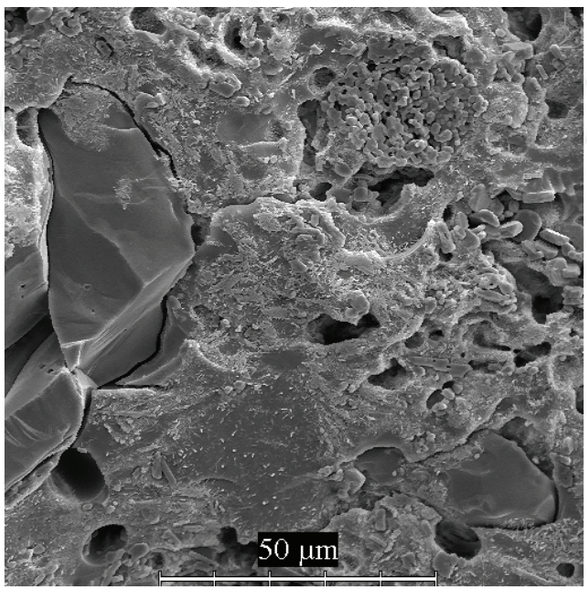

Fig. 10. Fracture surface with quartz grains and circumferential cracks around them. SEM after etching with 2.5 % HF for 15 s. Courtesy of PPC Čab

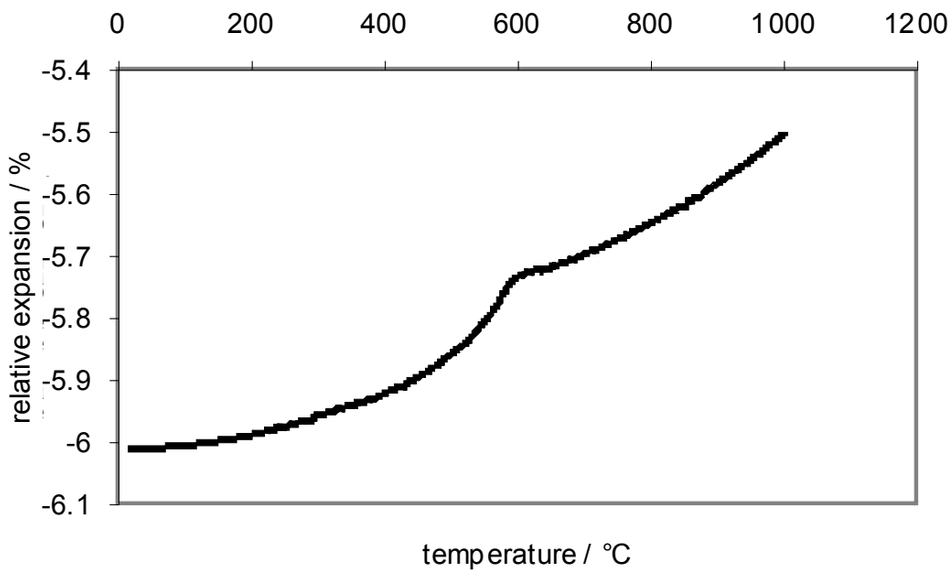

Fig. 11. Thermodilatometric curve of porcelain during cooling stage of firing

Results obtained using the real time non-destructive methods applied during the cooling stage of firing offer another view on the cracking process. An acoustic emission measurement directly registers the formation of the microcracks, and mf-TMA, which measures YM (or sound velocity), is sensitive to the concentration of the microcracks. The acoustic emission was employed in [26] to examine spontaneous cracking in porcelain samples during cooling. Acoustic emission signals were detected in the temperature range of 900 – 800 °C and never at temperatures less than 600 °C. These results were indirectly confirmed in [27] through measuring the sound velocity. Beside that, a decrease in the sound velocity below 570 °C was observed and assigned to the microcracks.

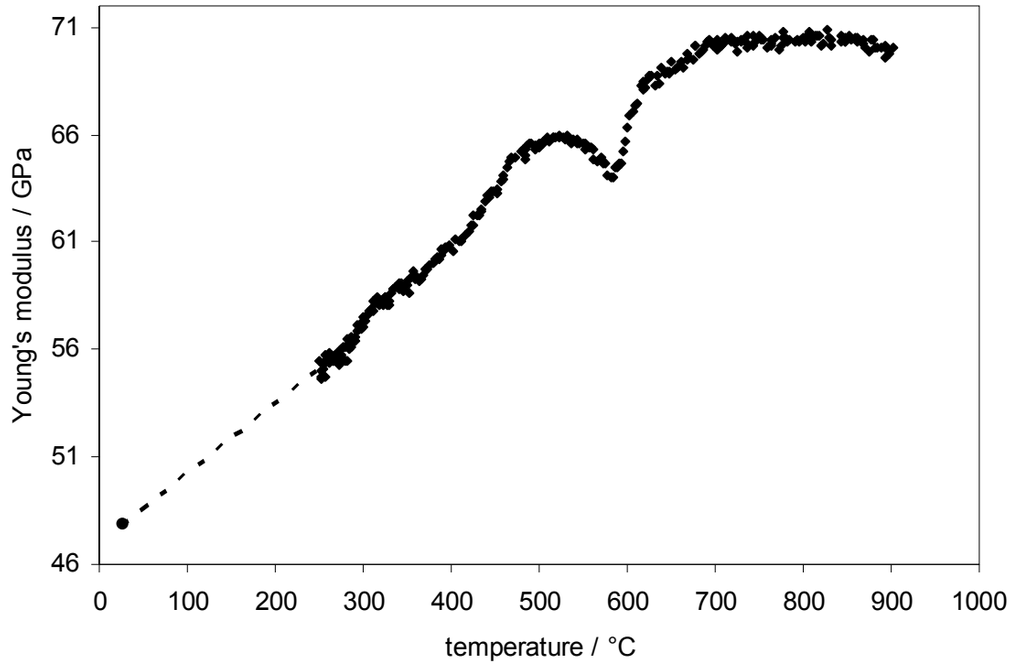

Fig. 12. Relationship between Young's modulus and temperature of green quartz sample during cooling stage of firing from max. temperature 1250 °C

A resonant flexural vibration develops in the sample if viscosity of the glassy phase is high enough for propagation of the mechanical flexural wave. This condition appears during cooling at the temperature of ~1000 °C. The relationship between YM and the temperature during cooling is depicted in Fig. 12. Values of YM increase with a decreasing temperature as long as the viscosity of the glassy phase is low enough to accommodate the mechanical stress generated during cooling. Subsequently, creation of microcracks may begin as a consequence of releasing the stress between phases with different thermal expansion coefficients. This process is demonstrated through descending values of YM below ~750 °C. Then there is a rapid decrease in the values with a sharp minimum at ~580 °C, which belongs to the $\beta \rightarrow \alpha$ quartz transition. During the further temperature decrease, there is a moderate and temporary recovery of Young's modulus values, followed by their restored drop from 500 °C to room temperature. This behavior supports results from the acoustic emission measurement. Intense acoustic signals, connected with the crack creation, were observed from ~800 °C to ~650 °C, then no signals appeared between 600 °C – 500 °C and

weak signals appeared again below 500 °C [28]. Consequently, most of the cracks in the vicinity of the quartz grains are created before the β → α transition and not during this transition as commonly believed.

Crack creation around the unsolved quartz grain can be caused by mechanical stress. According to [19], the total stress σ acting on the quartz particle may be calculated as

$$\sigma = \frac{\Delta\alpha \Delta T}{\frac{1+\mu_g}{2E_g} + \frac{1-2\mu_q}{E_q}} \tag{6}$$

where $\Delta\alpha = \alpha_g - \alpha_q$ is the difference between the thermal expansion coefficients of the glassy matrix and the quartz grain, and ΔT is the temperature range of the cooling process. E_g and E_q are Young's moduli of the glassy matrix and the quartz grain, respectively, and μ_g and μ_q are their Poisson's ratios. The thermodilatometric curves of the quartz and glassy phase and mullite (the last two curves are approximately identical according [26]) are depicted in Fig. 13. As can be deduced from Fig. 13, the quartz grain volume is almost constant and its glassy surrounding contracts its volume during cooling from 1000 °C to 570 °C. The stress applied on the grain according to Eq. (6) is positive (i.e. compressive stress). The glassy phase is under the tensile stress. Below the glass transformation temperature, the glassy matrix becomes brittle, which could result in formation of radial cracks nucleating at the quartz particles [19]. The nucleation and the growth of cracks are demonstrated by the decreasing values of Young's modulus (Fig. 12) below 800 °C. This process is finished by the β → α transition accompanied by a fast decrease in the thermal expansion of the quartz grains.

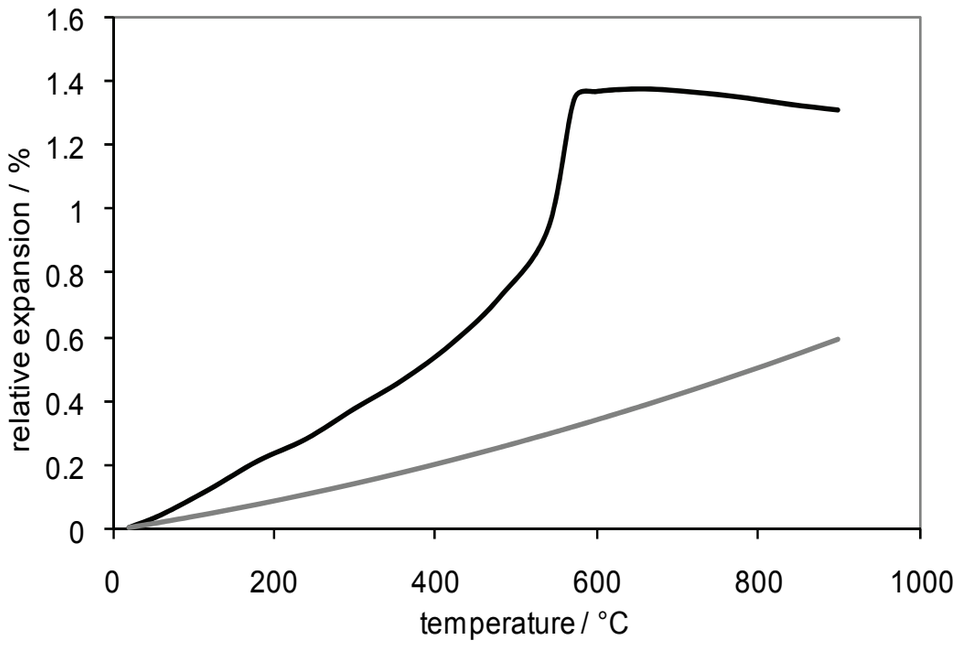

Fig. 13. Thermodilatometric curves of quartz (black line, main values from the curves for c-axis and a-axis [29]) and mullite [30] or glassy phase (gray line)

During the β → α transition of quartz, the contraction of the quartz phase volume proceeds faster than the contraction of the glassy phase, i.e. $\alpha_q > \alpha_g$ and the stress applied on the quartz grains becomes negative according to Eq. (6). During this fast process the tensile stress applied on the glassy matrix was rapidly relaxed, and upon further cooling, the compressive stress built up. This process took place between 573 and 500 °C, demonstrating itself by vanishing of acoustic signals (no new cracks nucleated) and a partial recovery of Young's modulus, likely due to the shrinkage of voids caused by previous cracking.
Below 500 °C, the relation $\alpha_q > \alpha_g$ continues to be valid until the room temperature is reached. After a short interval between 600 °C and 500 °C where no acoustic signals were detected [26, 28] and YM passed over a small maximum, YM continued to decrease its values and weak acoustic signals appeared again [28]. This can be explained by the newly built compressive stresses which induce an interface decohesion that takes the form of cracks around the quartz grains. The acoustic signals disappear at temperatures below 300 °C, which indicates that no further cracking occurs and the ongoing decrease of Young's modulus is caused by the accretion of already existing cracks [28].

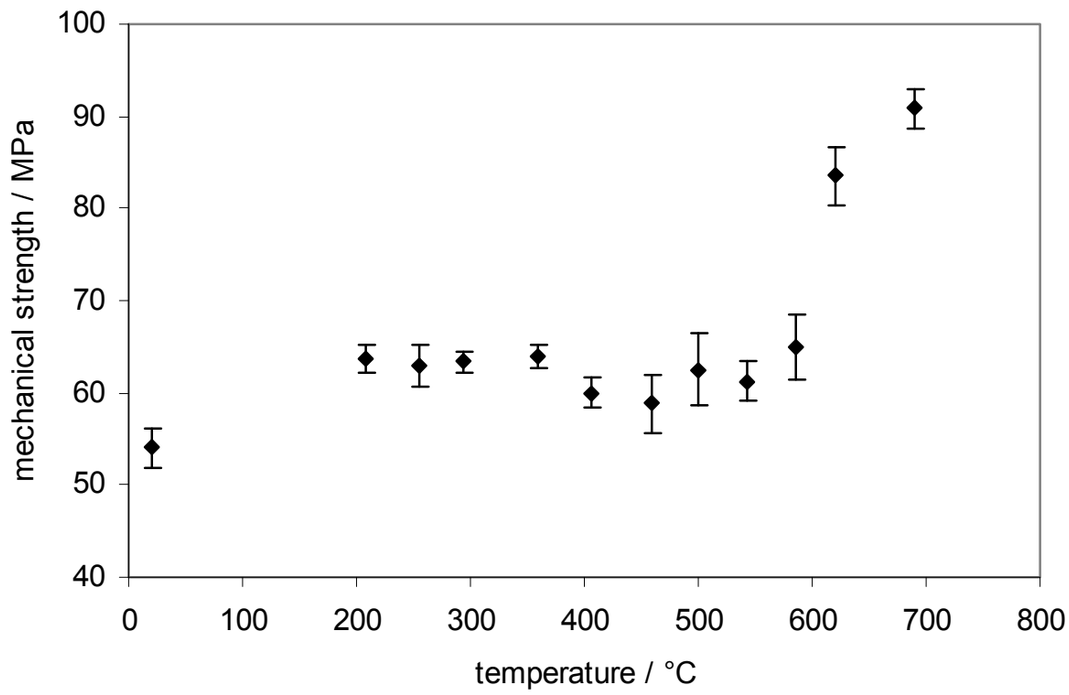

Fig. 14. Mechanical strength measured during cooling stage of the firing

The values of MOR measured in the cooling stage of firing, see Fig. 14, approximately confirm the conclusions shown above. MOR decreases before the β → α transition occurs, which is in agreement with the decreasing YM, and reaches the minimum at ~550 °C. A slightly higher value of MOR at 500 °C can be hardly considered a maximum, although it could correspond to the maximum of YM. Because of a few measured points in this region (450, 500, 550, 600 °C) and relatively large standard deviations of MOR, it is questionable to unambiguously relate the small increase in MOR at ~550 °C to a temporary recovery of YM.

The behavior of MOR and YM below 450 °C differs from the theoretical requirement of the direct proportion between these two quantities. The values of MOR initially increase (between 450 and 350 °C) and then remain constant up to 200 °C. On the other hand, YM decreases its values permanently. Both quantities, MOR and YM, reach their lowest values at room temperature.

5. Conclusions

Elastic properties (Young's modulus, sound velocity and mechanical strength) of the green quartz porcelain body reflect the changes in the structure of the body and the processes in it. They are linked to

a. escape of the physically bound water, dehydroxylation, the $\alpha \rightarrow \beta$ quartz transition, high-temperature reactions and solid-phase sintering during the heating stage of firing,
b. solidifying of the glassy phase, differences between the thermal expansion coefficients of the glassy phase, mullite and quartz grains, and the $\beta \rightarrow \alpha$ transition of quartz during the cooling stage of firing.

Results obtained by mf-TMA during heating showed a direct relationship between the elastic properties of kaolin and green porcelain samples. Young's modulus and the mechanical strength of the green porcelain sample seem to be determined by the properties of the interfaces between kaolinite crystals. Mechanical properties improve between 50 – 250 °C and then between 650 – 1100 °C, which can be explained by solid-phase sintering.

Young's modulus and the mechanical strength in the cooling stage of firing are predominantly determined by the stresses created and relaxed between the glassy phase and the quartz grains. They are a source of microcracks that are mostly located in the vicinity of the quartz grains. As a consequence, Young's modulus and the mechanical strength decrease.

Results obtained using the AE technique reveal several stages of microcracking. This process begins at the temperature of the glass transition. At the temperature of the $\beta \rightarrow \alpha$ transition, cracking is temporarily interrupted and a partial recovery of the structure occurs. Below this temperature circumferential cracks around the particles appear with less intensity, especially when the temperature is decreased below 300 °C.

6. Acknowledgment

This work was supported by the grant VEGA 1/0216/09, Ministry of Education of Slovakia. One of the authors (F.C.) gratefully acknowledges a financial support from the Research Goal MSM0021620834 that is financed by the Ministry of Education, Youth and Sports of the Czech Republic and from the research Grant 108/11/1267 financed by the Czech Science Foundation.

7. References

[1] Pospíšil, Z. – Koller, A.: *Fine Ceramics, Basics of Technology*. SNTL/ALFA, Praha 1981 (in Czech)
[2] Pytlík, P. – Sokolář, R.: *Building ceramics – technology, properties, applications*. Akad. nakladatelství CERM, Brno 2002 (in Czech)

[3] Norton, F.H.: *Fine ceramics – Technology and Application*. McGraw-Hill Book Co., New York 1970
[4] Hanykýř, V. – Kutzendorfer, J.: *Technology of Ceramics*. Silis Praha a Vega Hradec králové, Praha 2000 (in Czech)
[5] Palmour III, H.: Rate-controlled sintering of a whitware porcelain. *Ceramic Engineering and Science Proceedings*, 7, 1986, 1203-1212
[6] Štubňa, I. – Trník, A. – Vozár, L.: Thermomechanical and thermodilatometric analysis of green alumina porcelain. *Ceramics International*, 35, 2009, 1181-1185
[7] *ASTM C 848-88*: Standard test method for dynamic Young's modulus, shear modulus and Poisson's ratio for ceramic whiteware by sonic resonance. (published in 1999, Standard Documents, Philadelphia USA)
[8] *ASTM C 1198-01*: Standard test method for dynamic Young's modulus, shear modulus and Poisson's ratio for advanced ceramics by sonic resonance. (published in 2001, Standard Documents, Philadelphia USA)
[9] Schreiber, E. – Anderson, O. – Soga, N.: *Elastic constants and their measurement*. McGraw-Hill Book Co., New York 1973
[10] Štubňa, I. – Trník, A. – Vozár, L.: Determination of Young's modulus of ceramics from flexural vibration at elevated temperatures. *Acta Acustica + Acustica,* 97, 2011, 1-7
[11] Kashtaljan, J.A.: Elastic properties of materials at high temperatures. *Naukova dumka*, Kiev 1970 (in Russian)
[12] Rath, J. et al.: *Fine ceramics – measurement methods and testing*. SNTL/ALFA Praha, 1988 (in Czech)
[13] Polakovič, J. – Polakovičová, J. – Sokoly, J.: Interaction between kaolinite surface and hematoxyline. In: *Proc. 5th Meeting of European Clay Groups*, Prague, 1983, 279-282
[14] Kozík, T. – Rakovský, O. – Ondrejkovič, E.: Resistivity of ceramic material to thermal shock in dehydroxylation region. *Sklár a keramik*, 28, 1978, 176-180 (in Slovakian)
[15] Kozík, T. - Štubňa, I.: Mechanical strength of ceramic material in dehydroxylation region. *Silikáty*, 25, 1981, 237-241 (in Slovakian)
[16] Freund, F.: Kaolinite-metakaolinite, a model of a solid with extremely high lattice defect concentration. *Ber. Deutsche Keram. Ges.*, 44, 1967, 5-13
[17] Trník, A. – Štubňa, I. – Moravčíková, J.: Sound velocity of kaolin in the temperature range from 20 °C to 1100 °C. *International Journal of Thermophysics*, 30, 2009, 1323-1328
[18] Štubňa, I. – Trník, A. – Šín, P. – Sokolář, R.: Relationship between mechanical strength and Young's modulus in traditional ceramics. *Materiali in Tehnologije,* submitted article
[19] Carty, W.M. – Senapati, U.: Porcelain – raw materials, phase evolution, and mechanical behavior. *J. Amer. Ceram. Soc.*, 81, 1998, 3-20
[20] Liebermann, J.: About the important correlation between microstructure properties and product quality of strength-stressed high-voltage insulators. *Interceram*, 53, 2003, 238-241
[21] Liebermann, J.: Avoiding quartz in alumina porcelain for high-voltage insulators. *Keramische Zeitschrift*, 53, 2001, 683-686
[22] Liebermann, J.: Reliability of materials for high-voltage insulators. *www.ceramicbulletin.org*, (Amer. Ceram. Soc. Bulletin, May 2000)

[23] Porte, F. - Brydson, R. - Rand, B. - Riley, F.L.: Creep viscosity of vitreous china. *J. Amer. Ceram. Soc*., 87, 2004, 923-928

[24] Carty, W.M. – Pinto, B.M.: Effect of filler size on the strength of porcelain bodies. *Ceram. Engineering and Science Proceedings*, 23, 2002, 95-105

[25] Braganca, S.R. – Bergman, C.P.: Porcelain microstructure and technical properties. *Cerãmica*, 50, 2004, 291-299

[26] Ohya, Y. – Takahashi, Y.: Acoustic emission from a porcelain body during cooling. *J. Amer. Ceram. Soc*., 82, 1999, 445-448

[27] Štubňa, I. – Trník, A. – Vozár, L.: Thermomechanical analysis of quartz porcelain in temperature cycles. *Ceramics International*, 33, 2007, 1287-1291

[28] Chmelík, F. –Trník, A. – Pešička, J. – Štubňa, I.: Creation of microcracks in porcelain during firing. *J. of the European Ceramic Society* (accepted article)

[29] Prjanishnikov, V.P.: *Sistema kremnezema*. Izd. lit. po stroitelstvu, Leningrad 1971 (in Russian)

[30] Pena, B. – Bartolomé, J. – Requena, J. – Moya, J.S.: Mullite-alumina functionally gradient ceramics, *J. Physique IV*, 1993, 3, 1261-1266

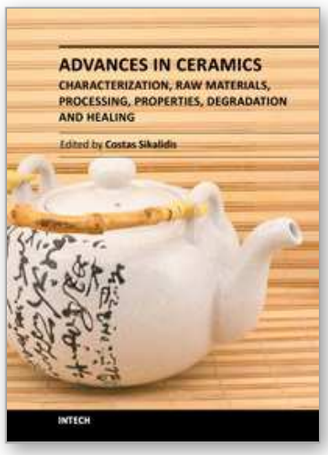

Advances in Ceramics - Characterization, Raw Materials, Processing, Properties, Degradation and Healing

Edited by Prof. Costas Sikalidis

ISBN 978-953-307-504-4
Hard cover, 370 pages
Publisher InTech
Published online 01, August, 2011
Published in print edition August, 2011

The current book consists of eighteen chapters divided into three sections. Section I includes nine topics in characterization techniques and evaluation of advanced ceramics dealing with newly developed photothermal, ultrasonic and ion spattering techniques, the neutron irradiation and the properties of ceramics, the existence of a polytypic multi-structured boron carbide, the oxygen isotope exchange between gases and nanoscale oxides and the evaluation of perovskite structures ceramics for sensors and ultrasonic applications. Section II includes six topics in raw materials, processes and mechanical and other properties of conventional and advanced ceramic materials, dealing with the evaluation of local raw materials and various types and forms of wastes for ceramics production, the effect of production parameters on ceramic properties, the evaluation of dental ceramics through application parameters and the reinforcement of ceramics by fibers. Section III, includes three topics in degradation, aging and healing of ceramic materials, dealing with the effect of granite waste addition on artificial and natural degradation bricks, the effect of aging, micro-voids, and self-healing on mechanical properties of glass ceramics and the crack-healing ability of structural ceramics.

How to reference

In order to correctly reference this scholarly work, feel free to copy and paste the following:

Igor Štubňa, Anton Trník, František Chmelík and Libor Vozár (2011). Mechanical Properties of Kaolin-Base Ceramics During Firing, Advances in Ceramics - Characterization, Raw Materials, Processing, Properties, Degradation and Healing, Prof. Costas Sikalidis (Ed.), ISBN: 978-953-307-504-4, InTech, Available from: http://www.intechopen.com/books/advances-in-ceramics-characterization-raw-materials-processing-properties-degradation-and-healing/mechanical-properties-of-kaolin-base-ceramics-during-firing

INTECH
open science | open minds

InTech Europe
University Campus STeP Ri
Slavka Krautzeka 83/A
51000 Rijeka, Croatia
Phone: +385 (51) 770 447
Fax: +385 (51) 686 166
www.intechopen.com

InTech China
Unit 405, Office Block, Hotel Equatorial Shanghai
No.65, Yan An Road (West), Shanghai, 200040, China
中国上海市延安西路65号上海国际贵都大饭店办公楼405单元
Phone: +86-21-62489820
Fax: +86-21-62489821

IntechOpen